RESEARCH ARTICLE

A Mouse Model for *Betacoronavirus* Subgroup 2c Using a Bat Coronavirus Strain HKU5 Variant

Sudhakar Agnihothram,[a] Boyd L. Yount, Jr.,[a] Eric F. Donaldson,[a] Jeremy Huynh,[a] Vineet D. Menachery,[a] Lisa E. Gralinski,[a] Rachel L. Graham,[a] Michelle M. Becker,[b] Sakshi Tomar,[d] Trevor D. Scobey,[a] Heather L. Osswald,[e] Alan Whitmore,[a] Robin Gopal,[c] Arun K. Ghosh,[e] Andrew Mesecar,[d] Maria Zambon,[c] Mark Heise,[a] Mark R. Denison,[b] Ralph S. Baric[a]

Departments of Epidemiology and Microbiology and Immunology, University of North Carolina, Chapel Hill, North Carolina, USA[a]; Departments of Pediatrics and Pathology and Microbiology and Immunology, Vanderbilt University, Nashville, Tennessee, USA[b]; Viral Zoonosis Unit, Public Health of England, London, United Kingdom[c]; Department of Chemistry, Purdue University, West Lafayette, Indiana, USA[d]; Departments of Chemistry and Medicinal Chemistry, Purdue University, West Lafayette, Indiana, USA[e]

ABSTRACT **Cross-species transmission of zoonotic coronaviruses (CoVs) can result in pandemic disease outbreaks. Middle East respiratory syndrome CoV (MERS-CoV), identified in 2012, has caused 182 cases to date, with ~43% mortality, and no small animal model has been reported. MERS-CoV and *Pipistrellus* bat coronavirus (BtCoV) strain HKU5 of *Betacoronavirus* (β-CoV) subgroup 2c share >65% identity at the amino acid level in several regions, including nonstructural protein 5 (nsp5) and the nucleocapsid (N) protein, which are significant drug and vaccine targets. BtCoV HKU5 has been described *in silico* but has not been shown to replicate in culture, thus hampering drug and vaccine studies against subgroup 2c β-CoVs. We report the synthetic reconstruction and testing of BtCoV HKU5 containing the severe acute respiratory syndrome (SARS)-CoV spike (S) glycoprotein ectodomain (BtCoV HKU5-SE). This virus replicates efficiently in cell culture and in young and aged mice, where the virus targets airway and alveolar epithelial cells. Unlike some subgroup 2b SARS-CoV vaccines that elicit a strong eosinophilia following challenge, we demonstrate that BtCoV HKU5 and MERS-CoV N-expressing Venezuelan equine encephalitis virus replicon particle (VRP) vaccines do not cause extensive eosinophilia following BtCoV HKU5-SE challenge. Passage of BtCoV HKU5-SE in young mice resulted in enhanced virulence, causing 20% weight loss, diffuse alveolar damage, and hyaline membrane formation in aged mice. Passaged virus was characterized by mutations in the nsp13, nsp14, open reading frame 5 (ORF5) and M genes. Finally, we identified an inhibitor active against the nsp5 proteases of subgroup 2c β-CoVs. Synthetic-genome platforms capable of reconstituting emerging zoonotic viral pathogens or their phylogenetic relatives provide new strategies for identifying broad-based therapeutics, evaluating vaccine outcomes, and studying viral pathogenesis.**

IMPORTANCE **The 2012 outbreak of MERS-CoV raises the specter of another global epidemic, similar to the 2003 SARS-CoV epidemic. MERS-CoV is related to BtCoV HKU5 in target regions that are essential for drug and vaccine testing. Because no small animal model exists to evaluate MERS-CoV pathogenesis or to test vaccines, we constructed a recombinant BtCoV HKU5 that expressed a region of the SARS-CoV spike (S) glycoprotein, thereby allowing the recombinant virus to grow in cell culture and in mice. We show that this recombinant virus targets airway epithelial cells and causes disease in aged mice. We use this platform to (i) identify a broad-spectrum antiviral that can potentially inhibit viruses closely related to MERS-CoV, (ii) demonstrate the absence of increased eosinophilic immune pathology for MERS-CoV N protein-based vaccines, and (iii) mouse adapt this virus to identify viral genetic determinants of cross-species transmission and virulence. This study holds significance as a strategy to control newly emerging viruses.**

Received 19 February 2014 **Accepted** 21 February 2014 **Published** 25 March 2014

Citation Agnihothram S, Yount BL, Jr, Donaldson EF, Huynh J, Menachery VD, Gralinski LE, Graham RL, Becker MM, Tomar S, Scobey TD, Osswald HL, Whitmore A, Gopal R, Ghosh AK, Mesecar A, Zambon M, Heise M, Denison MR, Baric RS. 2014. A mouse model for *Betacoronavirus* subgroup 2c using a bat coronavirus strain HKU5 variant. mBio 5(2): e00047-14. doi:10.1128/mBio.00047-14.

Editor W. Ian Lipkin, Columbia University

Address correspondence to Ralph S. Baric, rbaric@email.unc.edu.

Rapid response strategies for understanding emerging viral pathogenesis, testing vaccines and therapeutics that can restrict epidemic spread, and preventing morbidity and mortality are essential during the early phases of an epidemic. H5N1 and H7N9 influenza viruses and coronaviruses (CoVs) are emerging human pathogens that cause severe respiratory infections, often culminating in acute respiratory distress syndrome (ARDS), an end-stage lung disease associated with high mortality rates (1). CoVs are enveloped viruses belonging to the order *Nidovirales* and contain the largest known positive-sense RNA genome (~30 kb) (2). CoVs can replicate efficiently in a wide range of mammalian hosts and are divided into three major genera, *Alphacoronavirus*, *Betacoronavirus* (β-CoV), and *Gammacoronavirus*. Within these genera, CoVs are further divided into subgroups 1a and b, 2a to d, and 3 (3, 4). β-CoVs include human CoVs HKU1 and OC43, which cause mild to moderate respiratory disease, and the severe

acute respiratory syndrome coronavirus (SARS-CoV), which caused an epidemic in 2002 to 2003 that resulted in 10 to 50% age-dependent mortality (5, 6).

More recently, another β-CoV, called Middle East respiratory syndrome coronavirus (MERS-CoV), emerged in the Middle East in April of 2012, causing pneumonia and ARDS, as well as renal failure in some patients (7, 8). To date, MERS-CoV has spread to eight countries and has been implicated in 182 cases and 79 reported deaths, with mortality rates approaching 43%, especially in elderly patients (9). MERS-CoV shares a close phylogenetic relationship with the *Pipistrellus* bat coronavirus (BtCoV) strain HKU5 and *Tylonycteris* BtCoV strain HKU4; all three viruses are classified in β-CoV subgroup 2c (see Fig. S1A in the supplemental material) (7, 10). Bats can serve as reservoirs for circulating swarms of zoonotic viruses, and some are readily positioned to directly cross the species barrier and infect human populations (3, 4). SARS-CoV is believed to have originated from closely related bat predecessor strains similar to BtCoV HKU3, although the exact precursor virus has not been identified (3, 4, 11). While the zoonotic source of MERS-CoV remains unknown, recent reports identified the presence of β-CoVs with close amino acid similarity to MERS-CoV in *Nycteris* and *Pipistrellus* bat species (12, 13). Another study described the close similarity of MERS-CoV to BtCoV HKU5; both of these homologous viruses share high degrees of amino acid sequence similarity across important replicase protein targets, such as the 3C-like protease (3CLpro; also known as nonstructural protein 5 [nsp5]) (82%), polymerase (92%), and proofreading exonuclease (91%), as well as the nucleocapsid (N) protein (68%) (7, 10). A recent finding suggests that most of these proteins coevolve within subgroups of CoVs, making them attractive targets to test in models of closely related subgroups (14).

The lack of a small animal model for MERS-CoV has limited the understanding of the pathogenesis of β-CoVs belonging to subgroup 2c, thereby hampering the development of vaccines and therapeutics. BtCoV HKU5 shares a high degree of genetic sequence identity with MERS-CoV in the replicase targets and N genes. Therefore, developing a small animal model will assist us to identify viral determinants of pathogenesis and virulence, explore the possibility of vaccine-induced eosinophilia for MERS-CoV vaccines, and identify antivirals with broad activity against subgroup 2c strains. Furthermore, to date, no subgroup 2c bat CoVs have been cultured *in vitro*; the availability of infectious clones of these viruses will help us to dissect common evolutionary relationships among pathogenic CoV strains.

We report the *in vitro* reconstruction and biological characterization, using reverse genetics and synthetic-genome design, of an infectious clone of BtCoV HKU5 (icBtCoV HKU5) containing the ectodomain from the SARS spike (S) protein (BtCoV HKU5-SE). We show that BtCoV HKU5-SE replicated efficiently and demonstrate that a small molecule inhibitor targeting 3CLpro effectively inhibited BtCoV HKU5-SE and MERS-CoV replication in cell culture. In addition, we report that BtCoV HKU5-SE replicated to high titers in both young and aged mice but did not cause life-threatening disease. Virus replication and disease were dependent on the presence of the mouse angiotensin-converting enzyme 2 (ACE2) receptor, and immunohistochemistry staining demonstrated the presence of viral antigen in epithelial cells lining the small airways and alveoli. BtCoV HKU5-SE replication was inhibited by SARS-CoV S protein-based vaccines but was not sensitive to vaccines based on S proteins from subgroup 2c CoVs. Unlike mice vaccinated with SARS-CoV N-expressing Venezuelan equine encephalitis (VEE) virus replicon particles (VRP) (15), a severe eosinophilic immune pathology was not observed following BtCoV HKU5-SE challenge of animals vaccinated with VRP expressing HKU5 N or MERS-CoV N, supporting the development of killed and recombinant protein vaccines for MERS-CoV. *In vivo* passage of BtCoV HKU5-SE in young mice resulted in selection for a mouse-adapted strain (BtCoV HKU5-SE MA) that replicated more efficiently and caused significant clinical disease that progressed to interstitial pneumonia and diffuse alveolar damage (DAD) in aged mice. Mutations in nsp13, nsp14, open reading frame 5 (ORF5), and the M protein conferred increased virulence in mice. Taken together, our results illustrate the utility of synthetic-genomics-based platforms for rapidly generating a set of related zoonotic viruses, identifying viral determinants of increased virulence, assisting in the development of broadly active drugs, and previewing potential vaccine-related complications, which could provide invaluable directions for investigations during the early phases of an epidemic.

RESULTS

Synthetic reconstruction of BtCoV HKU5. We have previously described the synthetic reconstruction of a noncultivatable virus, BtCoV HKU3 (16). As phylogenetic studies indicate that BtCoV HKU5 is most closely related to MERS-CoV, we used published sequence information to synthesize an infectious molecular clone for BtCoV HKU5 (icBtCoV HKU5) (16, 17). The genome of the virus was synthesized as six contiguous cDNA fragments, as shown in Fig. 1A, and each subclone was flanked by class II restriction endonucleases that allow for directed assembly of a full-length cDNA genome, which encodes a T7 start at the 5′ end and a poly(T) tract at the 3′ end. Full-length RNAs were generated using *in vitro* transcription of ligated cDNAs (16, 18). Upon electroporation of Vero cells with the full-length RNA, no infectious virus was recoverable, despite robust expression of BtCoV HKU5 N subgenomic mRNAs through 4 days postelectroporation (see Fig. S1B in the supplemental material). Passage of cell culture supernatants resulted in diminished viral subgenomic N mRNA expression over time, and eventually, the recombinant virus went extinct in culture (Fig. S1C).

Recovery of an icBtCoV HKU5 variant expressing the ectodomain of the SARS-CoV S protein. Previous studies from our group and others demonstrated that substitution of the receptor binding domain (RBD) from the SARS-CoV S glycoprotein enabled efficient *in vivo* replication of BtCoV HKU3 (16, 19). To enable the recovery of BtCoV HKU5 in cell culture, we adopted a similar strategy and assembled a recombinant chimeric BtCoV HKU5 that encoded the S glycoprotein ectodomain (BtCoV HKU5-SE) (Fig. 1A; yellow) from SARS-CoV (16, 19). A Y436H substitution (change of Tyr to His at position 436) (Fig. 1A; asterisk), previously shown to enhance replication in mice (20), was also included in the spike gene. BtCoV HKU5-SE chimeric virus was recovered after electroporation of full-length transcripts into Vero cells.

Molecular characterization of BtCoV HKU5-SE. In Vero cells, BtCoV HKU5-SE replicated with kinetics similar to those of MERS-CoV (MERS-CoV SA1, the Saudi Arabian isolate) and SARS-CoV at earlier time points and achieved peak titers at 24 h p.i. (Fig. 1B and C). Cytopathology was characterized by fusion of

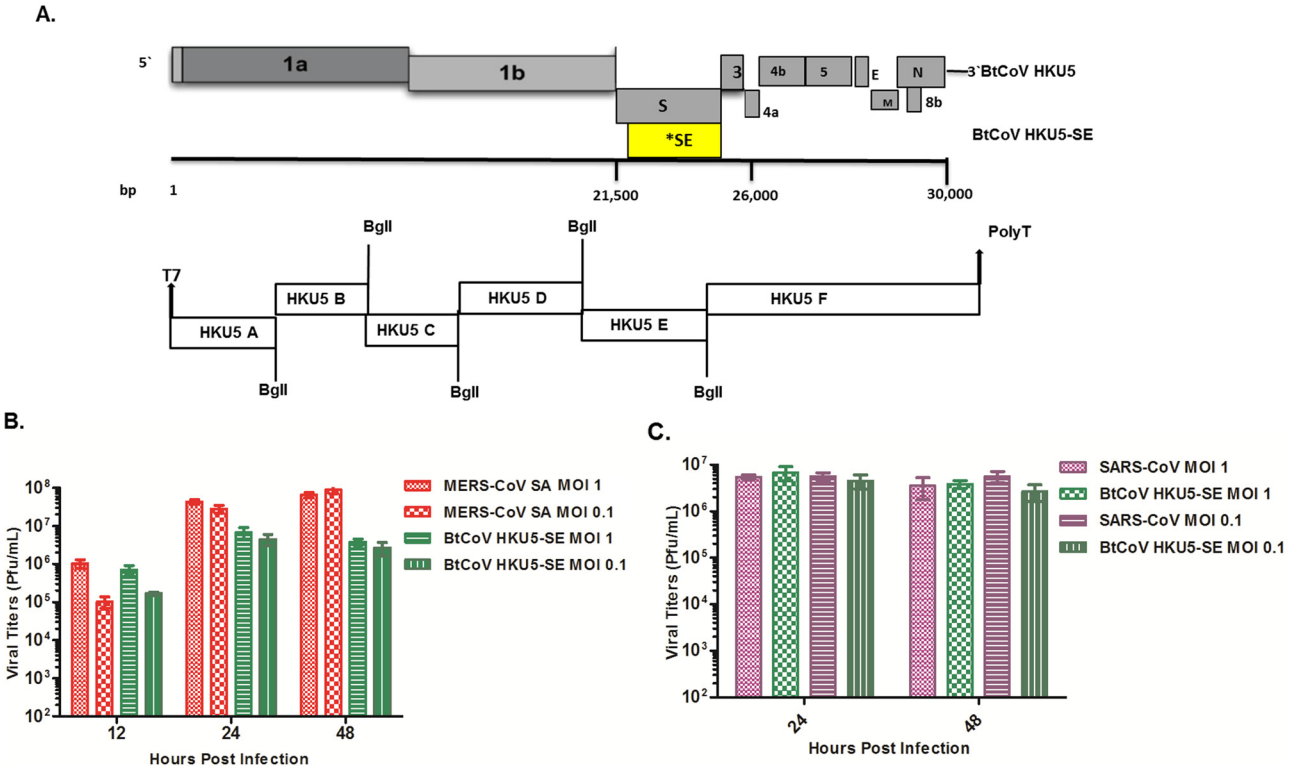

FIG 1 Genome organization and replication of BtCoV HKU5-SE in Vero cells. (A) Schematic of the genome organization of BtCoV HKU5 (top) and the recombinant virus in which the S protein was replaced with the ectodomain of SARS S glycoprotein (SE, yellow). The asterisk indicates the Y436H substitution. The bottom panel represents cDNA fragments A to F encoding the genome, with the T7 start site, the poly(T) tract, and the BglI restriction sites flanking the fragments. (B and C) BtCoV HKU5-SE replication in Vero cells compared with the replication of MERS-CoV Hu/SA-N1/2012 (MERS-CoV SA 1) (B) and SARS-CoV (C). Vero cells were infected with BtCoV HKU5-SE, MERS-CoV, and SARS-CoV at the indicated MOIs. Supernatants were sampled in triplicate at the times indicated, and titers determined on Vero cells by plaque assay. Error bars indicate standard deviations (SD).

cells starting at 18 h p.i., and cell death was noted at ~36 h p.i. BtCoV HKU5-SE was stable in cell culture, as indicated by real-time PCR analysis of ORF1 and ORF8 expression through passage six (see Fig. S1D in the supplemental material). BtCoV HKU5-SE replicated with kinetics similar to those of the MERS-CoV England isolate (MERS-CoV Eng 1) (Fig. S2A). Interestingly, there was a marked difference in virus replication (Fig. S2B) in high-level-ACE2-expressing H2B Calu-3 cells (a lung epithelial cell line), where BtCoV HKU5-SE replicated to lower titers than either MERS-CoV isolates or SARS-CoV. Although speculative, this growth difference is supported by low-level expression of N protein (Fig. S2C) at later time points and could reflect different sensitivities to interferon in Calu-3 cells.

Efficient CoV replication and transcription involves the production of a nested set of subgenomic mRNAs (2). Northern blot analysis from Vero cells infected with BtCoV HKU5-SE revealed eight subgenomic mRNAs (Fig. 2A). The predicted open reading frames encoded by each of the mRNAs are indicated in Table S1 in the supplemental material.

Next, we characterized the expression of structural proteins in cells infected with BtCoV HKU5-SE. Using antisera from mice vaccinated with VRPs expressing BtCoV HKU5 N protein, we demonstrated that BtCoV HKU5 infection of Vero cells produced a discrete N protein band at the predicted molecular mass of 50 kDa in cell lysates (Fig. 2B). Polyclonal serum specific for SARS-CoV S identified a 180-kDa S glycoprotein, along with a smaller S1 subunit (90 kDa, faster migrating band), in lysates from infected Vero cells (Fig. 2C), consistent with the expression of the SARS-CoV S ectodomain by the recombinant BtCoV HKU5-SE. In contrast, the polyclonal serum raised against BtCoV HKU5 S did not recognize the S protein (data not shown), supporting our earlier observations that the major antibody epitopes for S proteins are likely concentrated in the N terminus (21). The N protein of BtCoV HKU5 shares ~68% sequence identity with MERS-CoV and BtCoV HKU4 N proteins (7). To identify any possible cross-reactivity with BtCoV HKU5-SE, we generated mouse polyclonal sera using VRPs expressing the N proteins from BtCoV HKU4.2 and the MERS-CoV SA1 isolate and then demonstrated that these sera recognized the BtCoV HKU5-SE N protein (Fig. S2D and E). Taken together, these results demonstrate the presence of conserved polyclonal antibody epitopes in subgroup 2c CoV N proteins.

Protease inhibitors targeting MERS-CoV 3CLpro inhibit BtCoV HKU5-SE *in vitro*. Small molecule inhibitors targeting 3CLpro efficiently block SARS-CoV replication (22, 23). With the 82% sequence similarity between the nsp5 proteins of MERS-CoV and BtCoV HKU5-SE, we are well positioned to identify broadly reactive group 2c protease inhibitors, which is important because there are significant functional and regulatory differences in the nsp5 proteins of different subgroups (2a, 2b, and 2c) but strong conservation of determinants within subgroups (14).

Therefore, we analyzed whether the small molecule inhibitor

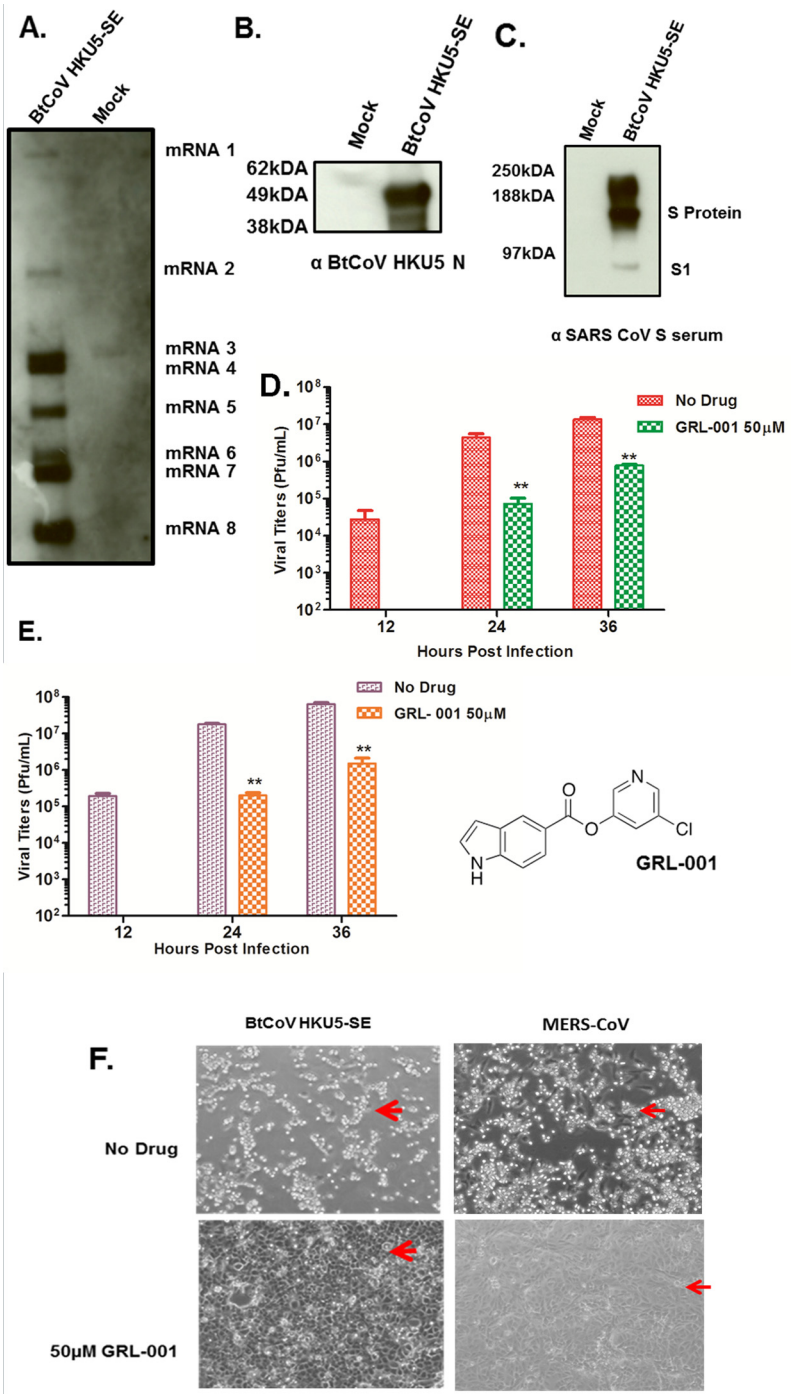

FIG 2 Subgenomic mRNA and protein expression in BtCoV HKU5-SE and the 3C-like protease inhibitor study. (A) Northern blot showing subgenomic mRNA expression in BtCoV HKU5-SE-infected cells. (B and C) Western blots showing expression of structural proteins N (B) and S (C) from BtCoV HKU5-SE-infected cell lysates stained with polyclonal serum as indicated below the images. (D and E) Viral titers from cells pretreated with 50 μM of GRL-001 and infected with BtCoV HKU5-SE (D) and MERS-CoV (E) at an MOI of 0.1 PFU/ml. Drug treatment was continued after infection, and virus-containing supernatants were sampled in triplicate. Error bars indicate SD. Asterisks indicate statistical significance ($P < 0.05$, Student *t* test). The structure of GRL-001 is shown to the right of panel E. (F) Bright-field images of cells infected with BtCoV HKU5-SE or MERS-CoV at an MOI of 0.1, showing strong cytopathic effects with no drug treatment (top, red arrows) and intact monolayers with 50 μM GRL-001 treatment (bottom, red arrows) at 36 h p.i..

GRL-001 could inhibit the replication of BtCoV HKU5-SE and MERS-CoV in cell culture (23, 24). The enzyme was purified using published methods (detailed in Methods in Text S1 in the supplemental material), resulting in high yield (28 mg/liter) and purity, and inhibition assays were conducted using a fluorimetric substrate as described previously (22, 23). GRL-001 was very potent in inhibiting BtCoV HKU5 3CLpro activity, with an inhibition constant (K_i) of 5.9 $\pm$ 0.8 μM (mean $\pm$ standard deviation). Vero cells pretreated with 50 μM concentrations of inhibitors were infected with BtCoV HKU5-SE or MERS-CoV at a multiplicity of infection (MOI) of 0.1, and viral titers were determined at 12, 24, and 36 h postinfection (p.i.). Importantly, GRL-001 completely blocked viral replication at early time points, reduced BtCoV HKU5-SE and MERS-CoV replication by ~100-fold at 24 h p.i. (Fig. 2D and E), and reduced virus-induced cytopathology in infected cells (Fig. 2F). Thus, GRL-001 is a small molecule inhibitor that effectively reduces the replication of multiple subgroup 2c CoV strains.

BtCoV HKU5-SE replication *in vivo*. To examine whether BtCoV HKU5-SE replicates and causes disease in mice, we intranasally infected young (~10-week-old) and old (1-year-old) BALB/c mice with 1×10^5 PFU of virus. BtCoV HKU5-SE did not cause weight loss in young animals, but aged BALB/c mice experienced ~10% weight loss by 4 days p.i. (Fig. 3A). In the aged-mouse model, clinical signs of disease included lethargy, ruffling of fur, and mildly labored breathing patterns. More importantly, in both young and aged mice, the virus replicated to 10^6 and $>10^4$ PFU/g in the lungs at 2 and 4 days p.i. (Fig. 3B). Weight loss and pathology changes were not noted in mock-infected young and aged animals (data not shown). Because the Y436H substitution in the SARS-CoV S ectodomain enhances binding to the mouse ACE2 receptor (20), we infected 1-year-old ACE2$^{-/-}$ mice with BtCoV HKU5-SE to assess whether ACE2 was required for virus entry and disease. No weight loss or virus replication was observed in ACE2$^{-/-}$ mice (Fig. 3A and B), clearly identifying the requirement of mouse ACE2 in BtCoV HKU5-SE entry, replication, and disease.

Although little if any pathology was noted in young infected animals, aged

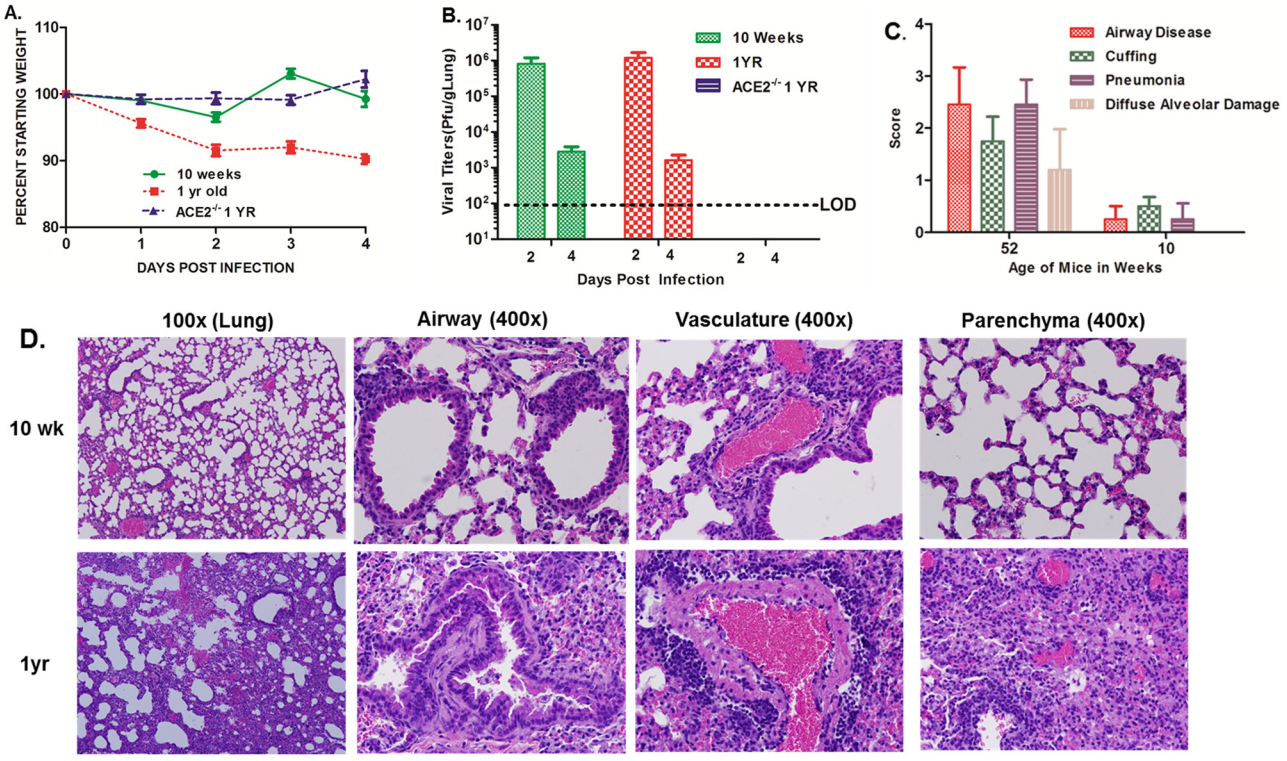

FIG 3 BtCoV HKU5-SE replication in BALB/c mice. (A) Weight loss in young (10-week-old) and aged (1-year-old) BALB/c mice and 1-year-old ACE2$^{-/-}$ mice (BALB/c background) was measured after intranasal infection with 1×10^5 PFU of BtCoV HKU5-SE. (B) Viral replication in mouse lungs at 2 and 4 days p.i. LOD, limit of detection. (C) Lung pathology from hematoxylin-and-eosin (H&E)-stained sections was blind scored for clinical disease features on a scale of 0 to 3 (1, mild; 3, severe). Error bars indicate SD. (D) Representative H&E-stained sections of lungs from a young and an aged mouse harvested at 4 days p.i., showing severe inflammatory infiltration in the aged mouse.

mice developed more-severe airway disease, perivascular and peribronchial cuffing, and pneumonia by 4 days p.i. The airway disease (Fig. 3C and D, bottom) included denuded regions of the airway epithelium, debris in the lumen of small airways, and peribronchial cuffing with increased numbers of neutrophils and monocytes. Perivascular cuffing was also evident, with large numbers of infiltrating neutrophils and monocytes. A few animals developed focal regions of severe pneumonia with accompanying edema-filled alveoli, consistent with early acute DAD (Fig. 3D, bottom). To identify cellular targets, immunohistochemistry with polyclonal serum to HKU5 N protein was performed in lung sections of young and aged mice. As seen with SARS-CoV (25), BtCoV HKU5-SE antigens were abundant in airway epithelial cells and in epithelial cells with features characteristic of type II pneumocytes in the alveoli (Fig. 4). No staining was noted in mock-infected lungs (Fig. 4, top and bottom, far right).

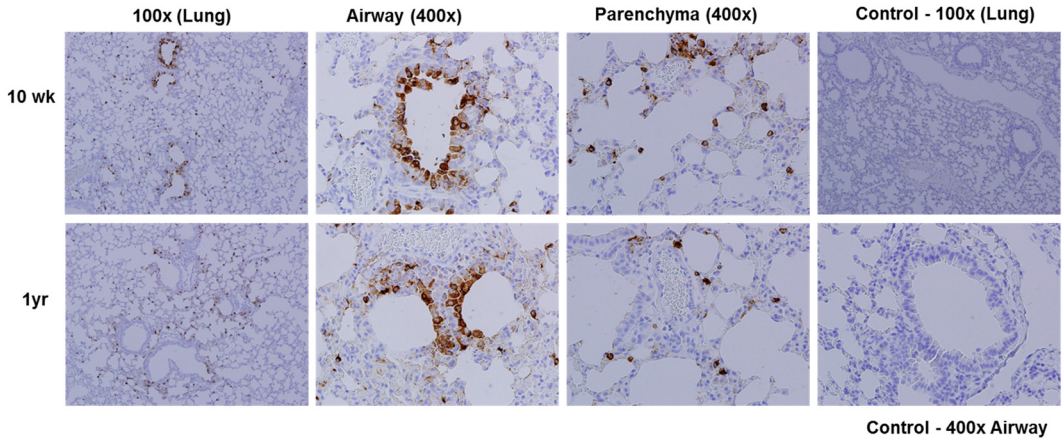

FIG 4 Viral antigen distribution in the lung. Immunohistochemistry was performed using anti-HKU5 N sera, and sections representing different regions of lungs from young and aged mice at 2 days p.i. are shown. Stained sections of lungs from mock-infected mice as controls are indicated on the extreme right in both rows.

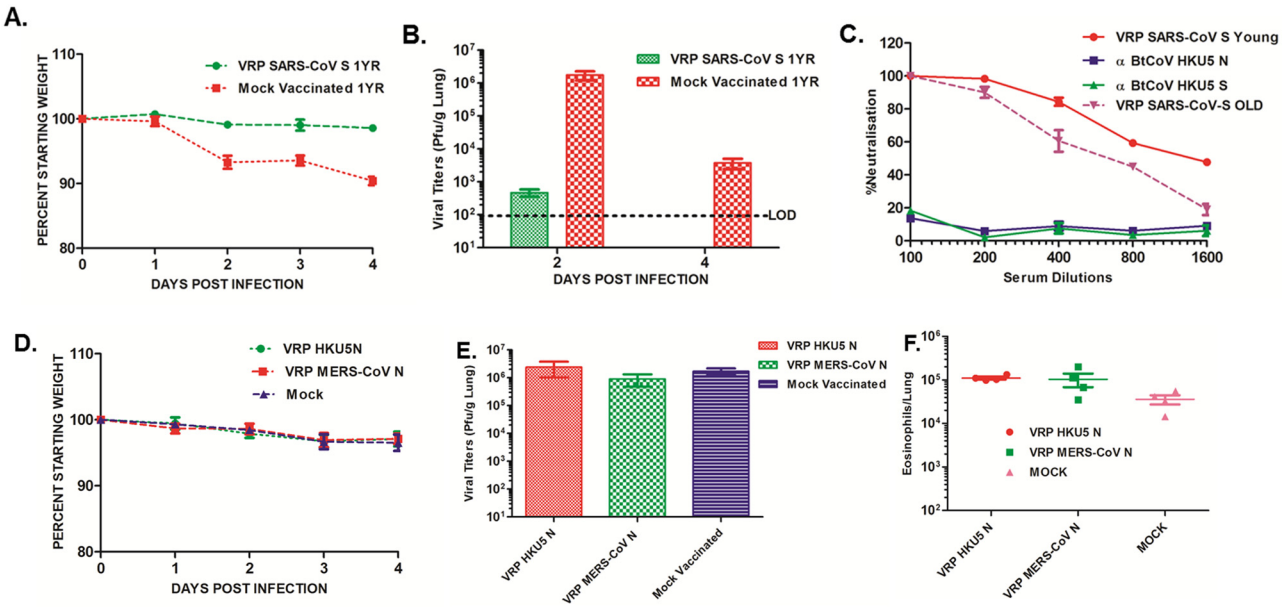

FIG 5 Vaccine studies in mice. (A) Weight loss of aged mice (1 year old) vaccinated with SARS-CoV S or mock vaccinated prior to challenge with 10^5 PFU of BtCoV HKU5-SE. (B) Virus titers in lungs at days 2 and 4 p.i. (C) Antiserum to SARS-CoV S protein but not antiserum to HKU5 S or N protein neutralizes BtCoV HKU5-SE in an *in vitro* $PRNT_{50}$ assay. (D) Weight loss of young mice either mock vaccinated or vaccinated with VRP (virus replicon particles) expressing HKU5 N or MERS-CoV N and challenged with BtCoV HKU5-SE. (E) Virus titers in lungs of mice at 2 days p.i. (F) Flow cytometric analysis showing numbers of eosinophils at 4 days p.i. in the lungs of mice either mock vaccinated or vaccinated with BtCoV HKU5 N or MERS-CoV N and then challenged with 10^5 PFU of BtCoV HKU5-SE. Error bars indicate SD.

S-expressing VRP vaccine studies in mice. Because BtCoV HKU5-SE harbors the SARS-CoV S ectodomain, we evaluated whether a SARS-CoV S-expressing VRP-based vaccine would provide protection from virus-induced disease. Young and aged mice were mock vaccinated (with VEE virus adjuvanted particles [VAP]) or vaccinated with VRP expressing SARS-CoV S glycoprotein and then challenged with 10^5 PFU of BtCoV HKU5-SE. Vaccinated aged animals were completely protected from virus-induced weight loss (Fig. 5A), and viral replication in the lungs was significantly diminished (~4 log) by day 2 and cleared by 4 days p.i. (Fig. 5B). In contrast, viral replication was not detected in young mice vaccinated with SARS-CoV S-expressing VRP (see Fig. S3A in the supplemental material), demonstrating complete protection. Consistent with this observation, the 50% plaque reduction neutralization test ($PRNT_{50}$) titers (against BtCoV HKU5-SE) in vaccinated young and aged animals were 1:1,600 and 1:800, respectively (Fig. 5C). Furthermore, polyclonal sera against HKU5 N and S proteins did not neutralize BtCoV HKU5-SE (Fig. 5C). These results are consistent with the idea that CoV S but not N proteins represent the principal determinants of protective humoral immunity after high-titer challenge (15).

We then determined whether VRP vaccines expressing the S proteins of other group 2c β-CoVs (BtCoV HKU4 or HKU5 or MERS-CoV) provided cross-protection against BtCoV HKU5-SE replication *in vivo*. Analysis of viral replication at 2 days p.i. indicated that none of these vaccines elicited cross-protection (see Fig. S3A in the supplemental material). Our results are consistent with a recent report showing the absence of cross-neutralization using SARS-CoV S-specific antibodies against full-length MERS-CoV S or its RBD (26).

Subgroup 2c N-based vaccines and immune pathology. Previous studies from our group and others have revealed immune-mediated pathology in the lungs of mice immunized with N protein-based subunit vaccines or doubly inactivated SARS-CoV vaccines and subsequently challenged with homologous or heterologous viruses (15, 27, 28). This immune-mediated pathology, as also noted with inactivated measles and respiratory syncytial virus (RSV) vaccines, was characterized by the presence of high numbers of pulmonary eosinophils after challenge and potentially poses a significant barrier in the development of vaccines against other emerging CoV infections (29, 30). Importantly, the BtCoV HKU5 N protein is 67% identical to MERS-CoV N and shares cross-reactive epitopes. As MERS-CoV does not replicate in mice, the BtCoV HKU5-SE recombinant virus offers a unique heterologous challenge model for assessing whether group 2c N protein-containing vaccines might elicit pulmonary immune pathology characterized by increased eosinophilia upon challenge.

Young mice were mock immunized (with VAP) or primed and boosted with VRP expressing MERS-CoV N or BtCoV HKU5 N and were subsequently challenged with BtCoV HKU5-SE. No appreciable weight loss was observed in any of the groups (Fig. 5D), and none of the vaccines provided protection from virus replication, as measured at 2 days p.i. (Fig. 5E). No significant increases in the numbers of eosinophils in lungs at 4 days p.i. were noted in mice immunized with either MERS-CoV N or BtCoV HKU5 N compared to the levels of eosinophils in lungs of mock-immunized animals ($P = 0.07$, as determined by Tukey's multiple-comparison test) (Fig. 5F). Analysis of histopathology sections also revealed no significant increases in the numbers of eosinophils between the mock-immunized and N protein-immunized groups (data not shown). No significant increases were noted for monocytes, monocyte-derived dendritic cells, or neutrophils between the N-vaccinated and mock-vaccinated groups either (see Fig. S3B to D in the supplemental material).

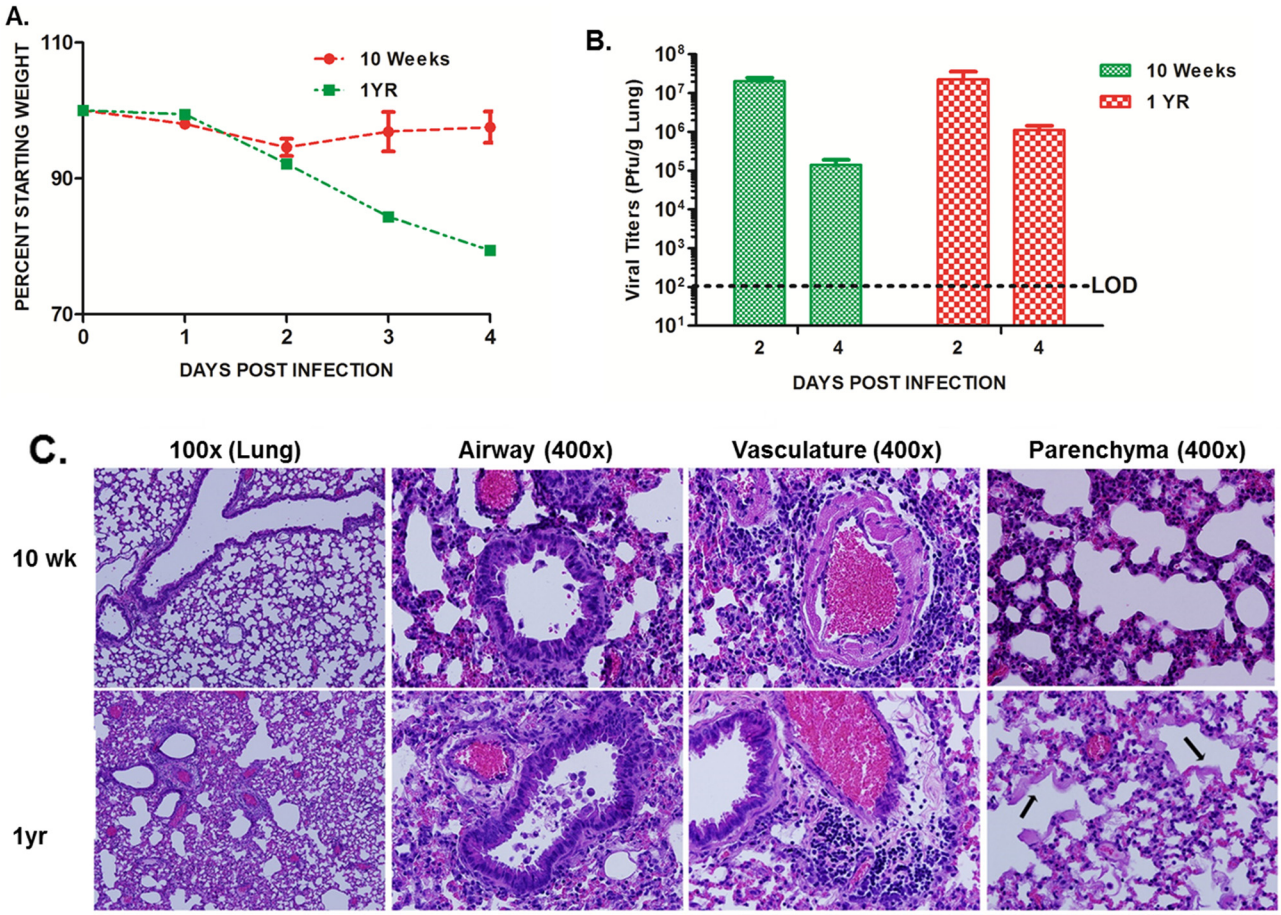

FIG 6 BtCoV HKU5-SE MA replication in young and aged BALB/c mice. (A) Weight loss curves of young (10-week-old) and aged (1-year-old) mice infected intranasally with 1×10^5 PFU of BtCoV HKU5-SE MA through 4 days p.i. (B) Viral titers in lungs of mice at days 2 and 4 p.i. Error bars indicate SD. (C) Representative H&E-stained sections of lungs from a young and an aged mouse harvested at 4 days p.i., showing severe inflammatory infiltration and hyaline membrane formation (black arrow) in the aged mouse.

However, there were significant increases in B cells ($P = 0.043$) and $CD8^+$ T cells ($P = 0.0002$) between the mock-immunized and N vaccine-immunized animals (Fig. S3E and F). Consistent with these findings, in a cell lysate-based enzyme-linked immunosorbent assay (ELISA), HKU5 N and MERS-CoV N sera bound to the appropriate recombinant proteins expressed by VRPs, indicating induction of antigen-specific antibodies (Fig. S4). Taken together, these results demonstrate that VRP-vectored HKU5 N- or MERS-CoV N-based vaccines do not elicit significant eosinophilia after homologous or heterologous challenge, supporting the development of MERS-CoV vaccines.

Mouse adaptation of BtCoV HKU5-SE. Although the S glycoprotein is a critical determinant for cross-species transmission, additional mutations across the genome have been shown to contribute to host switching and increased disease severity (20, 25). To identify potential virulence alleles in BtCoV HKU5-SE, we serially passaged BtCoV HKU5-SE in the lungs of 10-week-old BALB/c mice over 2-day intervals. Virus from passage 9 (BtCoV HKU5-SE MA [mouse adapted]) was plaque purified and used to inoculate young (10-week-old) and aged (1-year-old) animals. BtCoV HKU5-SE MA did not cause any significant weight loss in young mice, but it caused >20% weight loss in aged mice (Fig. 6A). The virus titers in lungs were significantly increased in young and aged animals at days 2 and 4 p.i. ($>10^7$ PFU/g and ~10^6 PFU/g, respectively) (Fig. 6B). Although young animals did not exhibit any significant increases in pathology compared to that in mice inoculated with nonadapted strains (Fig. 3D), all aged animals developed acute interstitial pneumonia with fibrin deposition and hyaline membrane formation (Fig. 6C). Genome sequencing in comparison to the sequence of the parent virus revealed changes in the nsp13, nsp14, ORF5, and ORF7 (M) genes as a result of mouse adaptation (Fig. 7A and B, top). It was noteworthy that a frameshift mutation resulted in a truncated ORF5 polyprotein (insertion of nucleotide G between 26,897 and 26,898 bp) (Fig. 7B, top). Furthermore, virus was also detected in blood at 2 days p.i. (4×10^5 PFU/ml), but not in any other organs tested (brain, liver, and spleen) (Fig. 7B, bottom).

DISCUSSION

A recent study by Anthony et al. estimates the presence of approximately 320,000 different viruses circulating in mammalian zoonotic reservoirs that have the potential to cross the species barrier and to emerge as new human pathogens (13, 31). Among coronaviruses, high RNA recombination frequencies coupled with the existence of interchangeable S domains suggest that some zoonotic strains are likely poised for cross-species transmission events

A.

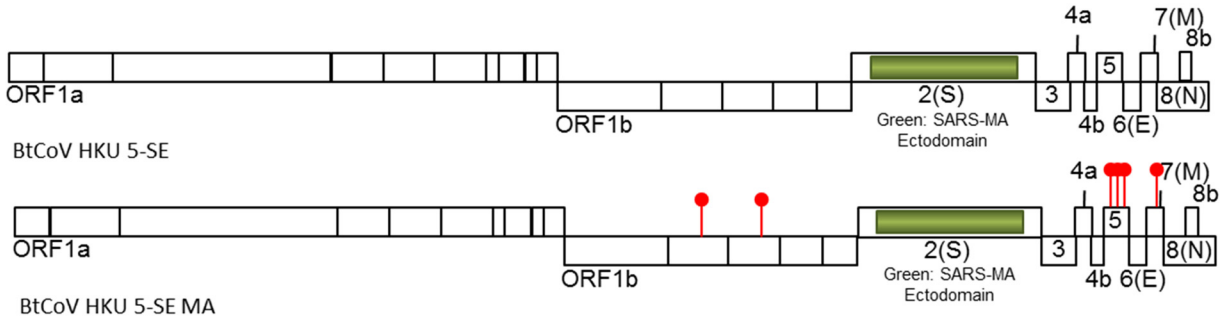

B.

Virus	Nucleotide Change	Affected Gene	Amino Acid Change
BtCoV HKU 5-SE MA	U17611G	nsp13	S431A
	A20116C	nsp14	T622P
	26897^26898 Ins G	ORF5	Truncation at 20 aa
	U27128C	ORF5	Past truncation
	G27332U	ORF5	Past truncation
	A28258U	ORF7	E135D

Organs or Body Fluids	Virus Titers at 2DPI	Virus Titers at 4 DPI
Brain	ND	ND
Liver	ND	ND
Spleen	ND	ND
Blood	$4*10^5$pfu/mL	ND

FIG 7 BtCoV HKU5-SE MA genome sequence. (A) Schematics of BtCoV HKU5-SE, depicting all open reading frames (ORFs) (top) and the mouse-adapted mutations as red stick-and-ball symbols at indicated spots in the genome (bottom). (B) Details of the mouse adaptations at the nucleotide and amino acid levels (top), and analysis of viremia in BtCoV HKU5-SE MA-infected aged (1-year-old) BALB/c mice (bottom).

into human populations (3). This study articulates a strategy that would enable rapid development of therapeutics and targeted evaluation of vaccines against future emerging zoonotic CoVs. A biopreparedness platform that includes panels of recombinant alpha-, beta-, and gammacoronaviruses for targeted therapeutic and vaccine evaluations can provide a strategy for rapidly identifying drugs with therapeutic potential against future emerging zoonotic CoVs. Previous studies have shown that the feline and murine S ectodomains and/or the S RBDs of the group 2b CoV S glycoproteins are interchangeable (16, 19). As preemergent SARS-like CoV group 2b strains with broad ACE2 receptor specificities have recently been isolated from bats (11), it seems likely that similar group 2c strains exist that have broad host range phenotypes as well. In addition, the antigenic distances and minimal cross-neutralization phenotypes seen across and within group 2b and 2c strains (21) demonstrate an inherent vulnerability in current vaccine and therapeutic design strategies, which focus on single emerging isolates for control purposes. Rather, the synthetic resurrection of the group 2b HKU3 strain Bat-SRBD (which has the spike RBD from SARS-CoV) (16) and, here, the MERS-CoV-like group 2c BtCoV HKU5-SE isolate provide crucial reagents for identifying broad-spectrum antivirals while addressing targeted issues in vaccine design. BtCoV HKU5 and MERS-CoV share high sequence identity across important replicase protein targets (7, 14, 32). As most zoonotic viruses are difficult to culture and usually exist as sequence signatures in repository databases, the advent of synthetic biology has provided an approach for resurrecting representative strains from these highly heterogeneous pools (16, 33, 34). Consequently, the potential risks versus benefits of these experiments and the plans for containment of the recombinant viruses were discussed in detail with the University of North Carolina Institutional Biosafety Committee in advance of these experiments.

Similar to our previous results with the subgroup 2b BtCoV strain HKU3 (16), the recombinant BtCoV HKU5 replicated but did not spread efficiently between cells, suggesting an entry block. This observation could reflect a low level or lack of appropriate receptor expression and/or other critical entry cofactors, such as cathepsins or TMPSSR2 proteases (35). Using a chimeric BtCoV HKU3 virus, we have previously demonstrated that the RBD of SARS-CoV S protein alone is sufficient for binding to mouse ACE2, enabling virus replication in mice (36). Inclusion of the mouse-adapted Y436H substitution in S (37) enhanced BtCoV HKU3 virus replication but not disease severity in aged-animal

models (16). In SARS-CoV recombinant viruses, S amino acid substitutions are sufficient to produce severe disease in aged BALB/c mouse models (20). In BtCoV HKU5, our attempts to replace the putative HKU5 RBD with the SARS-CoV RBD were unsuccessful, most likely reflecting the high antigenic distance and structural incompatibilities that hinder genetic exchange of some domains between subgroup 2b and 2c S glycoproteins. Supporting earlier work with mouse hepatitis virus and feline coronavirus (19), we introduced the SARS S glycoprotein ectodomain with the Y436H substitution into the BtCoV HKU5 genome (BtCoV HKU5-SE), and a recombinant chimeric virus was isolated that was capable of productive infection in culture and in young and aged BALB/c mice.

BtCoV HKU5-SE replicated efficiently in multiple cell types and used mouse ACE2 for entry into mice. The virus replication efficiency was reduced in interferon-competent Calu3 cells but not in Vero cells, similar to the results for SARS-CoV, suggesting the possibility of limited control by cell-intrinsic immune mechanisms as reported with SARS-CoV (38). Of interest, the ORF4b genes of group 2c strains like HKU5 and MERS-CoV are closely related and encode interferon antagonist activities, as detected using reporter assays (39). Using reverse genetics, our group and others have deleted these interferon antagonists from MERS-CoV (40, 41), with little to no effect on virus growth *in vitro*. The BtCoV HKU5-SE molecular clone would enable the dissection of related interferon antagonist activities in accessory ORFs of other group 2c CoVs, identifying common and unique pathways for regulating innate immune responses in human cells. It is noteworthy that ORF5 is not essential for the replication of either MERS-CoV or BtCoV HKU5-SE.

In infected cells, eight subgenomic mRNAs were detected by Northern blot assay, consistent with the predicted ORFs in GenBank and indicating successful replication and transcription. Most CoVs, including BtCoV HKU5, MERS-CoV, and SARS CoV, use a consensus ACGAA transcriptional regulatory sequence (TRS) start site, and the availability of a full panel of infectious clones will allow us to engineer a recombination- and reversion-proof genome by rewiring the TRS sites, as previously described by our group (42). The N and S glycoproteins were recognized by their respective polyclonal sera. Cross-reactivity was noted between BtCoV HKU5-SE, BtCoV HKU4, and MERS-CoV N proteins, demonstrating some conservation of antibody epitopes between the different strains. These data suggest that recombinant N proteins and N-specific antisera can be used as diagnostic reagents for serologic testing of human sera or direct detection of MERS-CoV and other group 2c CoV antigens in tissues.

The BtCoV HKU5-SE virus contains an authentic set of subgroup 2c replicase, accessory, and other structural proteins, providing a robust platform for evaluating the breadth of activity of antiviral drugs against the group 2c CoVs. Among the Coronaviridae, nsp5 (3CLpro) inhibitors have been shown to be successful in inhibiting SARS-CoV replication *in vitro* (22, 23). Using biochemical assays, the candidate drug GRL-001 inhibits MERS-CoV and BtCoV HKU5-SE nsp5 protease activity (24) and reduces MERS-CoV and BtCoV HKU5-SE replication by over 100-fold *in vitro*. Although an intact monolayer was observed in drug-treated cells at 36 h p.i., the virus titers were reduced only 10-fold. Similar differences have been reported for coronavirus papainlike protease (PLP) inhibitors (43). The drug might be slowing down the virus growth cycle and retarding the development of cytopathic effect (CPE). In addition to blocking the effects of 3CLpro, GRL-001 might interact with other host proteins activated during virus infection and prevent cell death. Nevertheless, its broad therapeutic action against distant group 2c CoVs supports the hypothesis that GRL-001 is an effective inhibitor of 3CLpro activities in multiple subgroup 2c CoVs, providing a potential candidate drug for future outbreaks. It is likely that GRL-001 will require modifications to improve its durability, biodistribution, and potency *in vivo*.

BtCoV HKU5-SE caused disease in aged but not young BALB/c mice, leading to 10% weight loss by 4 days p.i. In contrast to other coronaviruses, such as mouse hepatitis virus, which can still replicate and produce disease in carcinoembryonic antigen-related cell adhesion molecule 1-deficient (CEACAM1$^{-/-}$) animals (44), the replication and pathogenesis of BtCoV HKU5-SE was completely dependent upon the presence of the mouse ACE2 receptor, as the ACE2$^{-/-}$ mice clearly showed no weight loss or evidence of virus replication. Furthermore, the presence of viral antigen in small airway epithelial cells and in alveolar cells with morphology like type II pneumocytes is characteristic of tropisms reported during SARS-CoV infection in mice and primates (25, 45). Histopathologic examination demonstrated interstitial pneumonia in only a few aged animals, replicating phenotypes seen after infection with wild-type and mouse-adapted strains of SARS-CoV in humans and mice (20, 25). The basis for age-related disease phenotypes following SARS-CoV infection has been linked to alteration in prostaglandin expression in lungs that impairs dendritic cell migration, resulting in a diminished T cell response (46). Further studies are needed to evaluate the basis for the increased BtCoV HKU5-SE pathogenesis in the aged-animal models.

Mouse adaptation of BtCoV HKU5-SE resulted in increased viral replication and greater virulence in aged mice. Additionally, animals developed interstitial pneumonia with hyaline membrane formation. Mutations in nsp13, nsp14, ORF5, and ORF7 (M) genes were associated with increased virulence phenotypes in aged mice. Interestingly, evolution in the nsp13, nsp14, and M genes was also reported following SARS-CoV passage in mice (20, 25, 47) and humans during the expanding epidemic, which suggests that they play critical roles in cross-species adaptation, replication, and pathogenesis (48).

Importantly, the BtCoV HKU5-SE chimera was fully susceptible to a SARS-CoV S-based vaccine, and polyclonal serum raised against SARS-CoV S completely neutralized the virus *in vitro*. The difference in neutralization titers between young and aged animals likely reflects the gradient of immune response that occurs in aged animals following emerging CoV infections (49). These data demonstrate that the S glycoprotein retains key neutralization epitopes critical for protective immunity (16). In contrast, none of the VRPs expressing S proteins from BtCoV HKU4, BtCoV HKU5, or MERS-CoV conferred protection *in vivo*, demonstrating the divergence between other group 2b and 2c CoV S proteins. These findings argue that vaccine design for any novel emerging CoV should involve S protein from the respective virus or a chimeric multivalent vaccine containing neutralizing epitopes from the S proteins of different CoVs.

Previous studies from our laboratory and others have indicated that animals immunized with vectored or inactivated SARS-CoV N-containing vaccines develop an immune-mediated pathology in the lungs following homologous or heterologous challenge, reminiscent of RSV vaccine-mediated immune pathologies (27,

28). This immune pathology is characterized by high numbers of eosinophil infiltrates in the lungs postchallenge (28). Our results demonstrate that VRP vaccines expressing MERS-CoV N did not elicit an eosinophilic immune pathology following BtCoV HKU5-SE challenge, as reported with inactivated SARS-CoV vaccines (27). In contrast to alum, which causes a Th2-skewed immune response (27), VRP vaccines induce a robust Th1 immune response and high neutralizing antibody titers (15, 27). Although these studies should be interpreted with some caution, the effects of inactivated MERS-CoV and BtCoV HKU5-SE vaccines in induction of eosinophilia following challenge remain to be tested. VRP vectors have been proven successful in human clinical trials (50, 51), and VEE virus replicates successfully in several animal species, including horses, goats, and sheep (52). Given the high seroprevalence of MERS-CoV in camels and the potential role of camels as intermediate reservoirs for human disease (53), the VRP platform described here may be an effective MERS-CoV vaccine candidate for use in camels and other reservoir species.

The development of infectious clones and recombinant viruses from emerging zoonotic CoVs will expedite the rapid testing of antivirals and vaccines in an outbreak situation. A limitation of the current approach is that wild-type MERS-CoV and BtCoV HKU5 do not replicate in mice. The recent demonstration of the MERS-CoV S glycoprotein bound to its receptor may inspire strategies for designing recombinant MERS-CoV strains that replicate well in mice (54). Using BtCoV HKU5-SE, we illustrate the utility of synthetic genomics and reverse genetic strategies for resurrecting emerging zoonotic viruses *in vitro* and validate our findings using drugs and vaccines that can be readily applied in outbreak situations.

MATERIALS AND METHODS

Viruses, cells, and plaque assays. BtCoV HKU5-SE, MERS-CoV Hu/England-N1/2012, and MERS-CoV Hu/SA-N1/2012 were cultured on Vero 81 cells and grown in Dulbecco modified Eagle medium (Gibco, CA) with 5% Fetalclone II (Hyclone, South Logan, UT) and gentamicin-kanamycin (Gibco, Carlsbad, CA). Growth curves in Vero and Calu-3 cells were performed as previously described (55). All virus cultivation was performed in a biosafety level 3 (BSL3) laboratory with redundant fans in biosafety cabinets (18, 20). All personnel wore powered air-purifying respirators (3M Breathe Easy) and Tyvek suits, aprons, and booties and were double gloved.

Generation of polyclonal mouse antisera, neutralization assays, and Western and Northern blot analyses. Genes encoding the CoV S and N proteins indicated above were synthesized by Bio Basic, Inc. (Ontario, Canada) and were packaged into Venezuelan equine encephalitis (VEE) virus replicon particles (VRPs) under BSL2 conditions using attenuated VEE virus 3526 structural protein helpers. Following vaccination, mouse polyclonal sera were generated in BALB/c mice, and neutralization assays involving MERS-CoV isolates and SARS-CoV and using mouse antisera were performed as described previously (49). For Western blotting, lysates from cells infected with BtCoV HKU5-SE or MERS-CoV isolates were prepared at 12 h p.i. as described previously (36). The blots were then probed using the mouse polyclonal sera indicated above. Vero cells inoculated with BtCoV HKU5-SE were harvested at 12 h p.i. with TRizol reagent (Invitrogen). Northern blot analysis to describe the genome- and subgenome-length RNAs was performed using a probe for the N gene as described previously (37).

Systematic assembly and recovery of full-length infectious clones of BtCoV HKU5 variants. The BtCoV HKU5 molecular clone was designed based on a consensus sequence of BtCoV HKU5 isolates available in GenBank (nucleotide sequence accession number EF065512.1). The gene encoding the BtCoV HKU5 S protein (ORF2) was also replaced with the full-length ectodomain of the SARS-CoV S protein (residues 1 to 1190) using previously described strategies (16, 19). The mouse-adapted substitution Y436H in the SARS-CoV spike protein (20, 25) was also included in the chimeric S construct to promote replication in mice. This clone was designated BtCoV HKU5-SE. The wild-type virus and chimeric BtCoV HKU5 E fragments were synthesized by Bio Basic, Inc. (Ontario, Canada) as six contiguous cDNAs. After assembly and *in vitro* transcription, recombinant virus was recovered on Vero cells through transfection of the full-length transcripts, as previously described in detail (16, 18).

Biosafety statement. Synthetic reconstruction of BtCoV HKU5 and BtCoV HKU5-SE was approved by the University of North Carolina IBC (Institutional Biosafety Committee), which also reviewed possible dual use research concerns before these experiments were undertaken. The IBC also examined the manuscript before submission.

BtCoV HKU5-SE replication and serial passage in mice. Young (10-week-old) and aged (1-year-old) BALB/c mice purchased from Harlan Labs were intranasally inoculated with a 50-μl volume containing 1×10^5 PFU of BtCoV HKU5-SE virus. Infected animals were monitored for weight loss, morbidity, and clinical signs of disease, and lung titers were determined by plaque assay. Adaptation to mice was conferred by serial passage in lungs of young BALB/c mice (10 weeks old) at 2-day intervals p.i. as has been described in detail previously (25). Animal housing, care, and experimental protocols were in accordance with University of North Carolina Institutional Animal Care and Use Committee (IACUC) guidelines.

Immunohistochemistry. Lungs from mice infected with BtCoV HKU5-SE were harvested at 2 and 4 days p.i. in 10% formalin and were fixed for 7 days before removal from the BSL3. Paraffin-embedded tissues (5 μM) were sectioned and stained with hematoxylin and eosin stain, and lung sections were blind scored for pathological changes. Staining of viral antigens was performed as described previously (25), using polyclonal serum to the HKU5 N protein.

VRP-based S and N vaccination experiments. Young (~5- to 6-week-old) and aged (~1-year-old) mice received, in the left footpad, a prime and a boost of 10^5 PFU of different VRP-based S or N vaccines or Venezuelan equine encephalitis virus adjuvanted particles (VAP) which expressed no transgene as a mock-infection control, with a 3-week interval between the prime and the boost. At 3 weeks after the boost, the animals were moved into the BSL3 facility and allowed to acclimate for 1 week. Then, they were challenged with BtCoV HKU5-SE. All young animals were ~13 weeks, and aged animals were 14 months old at the time of challenge.

Flow cytometry. Young BALB/c mice that were mock immunized with 10^5 infectious units of VAP (expresses no transgene) or vaccinated with VRP encoding BtCoV HKU5 N or MERS-CoV N were challenged with 1×10^5 PFU of BtCoV HKU5-SE. The animals were weighed and monitored for clinical symptoms daily. On day 4 p.i., mice were sacrificed by isoflurane inhalation, and viable cell populations from the lungs were prepared, stained with appropriate antibodies, and sorted using flow cytometry as previously described in detail (27).

SUPPLEMENTAL MATERIAL

Supplemental material for this article may be found at http://mbio.asm.org/lookup/suppl/doi:10.1128/mBio.00047-14/-/DCSupplemental.

Text S1, PDF file, 0.2 MB.
Figure S1, PDF file, 2.4 MB.
Figure S2, PDF file, 0.8 MB.
Figure S3, PDF file, 1.9 MB.
Figure S4, PDF file, 0.2 MB.
Table S1, PDF file, 0.2 MB.

ACKNOWLEDGMENTS

This work was supported in part by grants from the National Institutes of Health (U19 AI107810 to R.S.B., AI108197 and U54 AI057157 to R.S.B. and M.R.D., and AI26603 to M.R.D. and A.M.).

REFERENCES

1. **Tsushima K, King LS, Aggarwal NR, De Gorordo A, D'Alessio FR, Kubo K.** 2009. Acute lung injury review. Intern. Med. **48:**621–630. http://dx.doi.org/10.2169/internalmedicine.48.1741.
2. **Masters PS.** 2006. The molecular biology of coronaviruses. Adv. Virus Res. **66:**193–292. http://dx.doi.org/10.1016/S0065-3527(06)66005-3.
3. **Graham RL, Baric RS.** 2010. Recombination, reservoirs, and the modular spike: mechanisms of coronavirus cross-species transmission. J. Virol. **84:**3134–3146. http://dx.doi.org/10.1128/JVI.01394-09.
4. **Bolles M, Donaldson E, Baric R.** 2011. SARS-CoV and emergent coronaviruses: viral determinants of interspecies transmission. Curr. Opin. Virol. **1:**624–634. http://dx.doi.org/10.1016/j.coviro.2011.10.012.
5. **Pyrc K, Sims AC, Dijkman R, Jebbink M, Long C, Deming D, Donaldson E, Vabret A, Baric R, van der Hoek L, Pickles R.** 2010. Culturing the unculturable: human coronavirus HKU1 infects, replicates, and produces progeny virions in human ciliated airway epithelial cell cultures. J. Virol. **84:**11255–11263. http://dx.doi.org/10.1128/JVI.00947-10.
6. **Rota PA, Oberste MS, Monroe SS, Nix WA, Campagnoli R, Icenogle JP, Peñaranda S, Bankamp B, Maher K, Chen MH, Tong S, Tamin A, Lowe L, Frace M, DeRisi JL, Chen Q, Wang D, Erdman DD, Peret TC, Burns C, Ksiazek TG, Rollin PE, Sanchez A, Liffick S, Holloway B, Limor J, McCaustland K, Olsen-Rasmussen M, Fouchier R, Günther S, Osterhaus AD, Drosten C, Pallansch MA, Anderson LJ, Bellini WJ.** 2003. Characterization of a novel coronavirus associated with severe acute respiratory syndrome. Science **300:**1394–1399. http://dx.doi.org/10.1126/science.1085952.
7. **van Boheemen S, de Graaf M, Lauber C, Bestebroer TM, Raj VS, Zaki AM, Osterhaus AD, Haagmans BL, Gorbalenya AE, Snijder EJ, Fouchier RA.** 2012. Genomic characterization of a newly discovered coronavirus associated with acute respiratory distress syndrome in humans. mBio **3**(6):e00473-12. http://dx.doi.org/10.1128/mBio.00473-12.
8. **Zaki AM, van Boheemen S, Bestebroer TM, Osterhaus AD, Fouchier RA.** 2012. Isolation of a novel coronavirus from a man with pneumonia in Saudi Arabia. N. Engl. J. Med. **367:**1814–1820. http://dx.doi.org/10.1056/NEJMoa1211721.
9. **Memish ZA, Zumla AI, Assiri A.** 2013. Middle East respiratory syndrome coronavirus infections in health care workers. N. Engl. J. Med. **369:**884–886.
10. **Lau SK, Li KS, Tsang AK, Lam CS, Ahmed S, Chen H, Chan KH, Woo PC, Yuen KY.** 2013. Genetic characterization of betacoronavirus lineage C viruses in bats revealed marked sequence divergence in the spike protein of Pipistrellus bat coronavirus HKU5 in Japanese pipistrelle: implications for the origin of the novel Middle East respiratory syndrome coronavirus. J. Virol. **87:**8638–8650. http://dx.doi.org/10.1128/JVI.01055-13.
11. **Ge XY, Li JL, Yang XL, Chmura AA, Zhu G, Epstein JH, Mazet JK, Hu B, Zhang W, Peng C, Zhang YJ, Luo CM, Tan B, Wang N, Zhu Y, Crameri G, Zhang SY, Wang LF, Daszak P, Shi ZL.** 2013. Isolation and characterization of a bat SARS-like coronavirus that uses the ACE2 receptor. Nature **503:**535–538. http://dx.doi.org/10.1038/nature12711.
12. **Annan A, Baldwin HJ, Corman VM, Klose SM, Owusu M, Nkrumah EE, Badu EK, Anti P, Agbenyega O, Meyer B, Oppong S, Sarkodie YA, Kalko EK, Lina PH, Godlevska EV, Reusken C, Seebens A, Gloza-Rausch F, Vallo P, Tschapka M, Drosten C, Drexler JF.** 2013. Human betacoronavirus 2c EMC/2012-related viruses in bats, Ghana and Europe. Emerg. Infect. Dis. **19:**456–459.
13. **Anthony SJ, Ojeda-Flores R, Rico-Chávez O, Navarrete-Macias I, Zambrana-Torrelio CM, Rostal MK, Epstein JH, Tipps T, Liang E, Sanchez-Leon M, Sotomayor-Bonilla J, Aguirre AA, Ávila-Flores R, Medellín RA, Goldstein T, Suzán G, Daszak P, Lipkin WI.** 2013. Coronaviruses in bats from Mexico. J. Gen. Virol. **94:**1028–1038. http://dx.doi.org/10.1099/vir.0.049759-0.
14. **Stobart CC, Sexton NR, Munjal H, Lu X, Molland KL, Tomar S, Mesecar AD, Denison MR.** 2013. Chimeric exchange of coronavirus nsp5 proteases (3CLpro) identifies common and divergent regulatory determinants of protease activity. J. Virol. **87:**12611–12618. http://dx.doi.org/10.1128/JVI.02050-13.
15. **Deming D, Sheahan T, Heise M, Yount B, Davis N, Sims A, Suthar M, Harkema J, Whitmore A, Pickles R, West A, Donaldson E, Curtis K, Johnston R, Baric R.** 2006. Vaccine efficacy in senescent mice challenged with recombinant SARS-CoV bearing epidemic and zoonotic spike variants. PLoS Med. **3:**e525. http://dx.doi.org/10.1371/journal.pmed.0030525.
16. **Becker MM, Graham RL, Donaldson EF, Rockx B, Sims AC, Sheahan T, Pickles RJ, Corti D, Johnston RE, Baric RS, Denison MR.** 2008. Synthetic recombinant bat SARS-like coronavirus is infectious in cultured cells and in mice. Proc. Natl. Acad. Sci. U. S. A. **105:**19944–19949. http://dx.doi.org/10.1073/pnas.0808116105.
17. **Donaldson EF, Yount B, Sims AC, Burkett S, Pickles RJ, Baric RS.** 2008. Systematic assembly of a full-length infectious clone of human coronavirus NL63. J. Virol. **82:**11948–11957. http://dx.doi.org/10.1128/JVI.01804-08.
18. **Yount B, Curtis KM, Fritz EA, Hensley LE, Jahrling PB, Prentice E, Denison MR, Geisbert TW, Baric RS.** 2003. Reverse genetics with a full-length infectious cDNA of severe acute respiratory syndrome coronavirus. Proc. Natl. Acad. Sci. U. S. A. **100:**12995–13000. http://dx.doi.org/10.1073/pnas.1735582100.
19. **de Haan CA, Haijema BJ, Masters PS, Rottier PJ.** 2008. Manipulation of the coronavirus genome using targeted RNA recombination with interspecies chimeric coronaviruses. Methods Mol. Biol. **454:**229–236. http://dx.doi.org/10.1007/978-1-59745-181-9_17.
20. **Frieman M, Yount B, Agnihothram S, Page C, Donaldson E, Roberts A, Vogel L, Woodruff B, Scorpio D, Subbarao K, Baric RS.** 2012. Molecular determinants of severe acute respiratory syndrome coronavirus pathogenesis and virulence in young and aged mouse models of human disease. J. Virol. **86:**884–897. http://dx.doi.org/10.1128/JVI.05957-11.
21. **Agnihothram S, Gopal R, Yount BL, Donaldson EF, Menachery VD, Graham RL, Scobey TD, Gralinski LE, Denison MR, Zambon M, Baric RS.** 2013. Evaluation of serologic and antigenic relationships between Middle Eastern respiratory syndrome coronavirus and other coronaviruses to develop vaccine platforms for the rapid response to emerging coronaviruses. J. Infect. Dis.. http://dx.doi.org/10.1093/infdis/jit609.
22. **Ratia K, Pegan S, Takayama J, Sleeman K, Coughlin M, Baliji S, Chaudhuri R, Fu W, Prabhakar BS, Johnson ME, Baker SC, Ghosh AK, Mesecar AD.** 2008. A noncovalent class of papain-like protease/deubiquitinase inhibitors blocks SARS virus replication. Proc. Natl. Acad. Sci. U. S. A. **105:**16119–16124. http://dx.doi.org/10.1073/pnas.0805240105.
23. **Ghosh AK, Gong G, Grum-Tokars V, Mulhearn DC, Baker SC, Coughlin M, Prabhakar BS, Sleeman K, Johnson ME, Mesecar AD.** 2008. Design, synthesis and antiviral efficacy of a series of potent chloropyridyl ester-derived SARS-CoV 3CLpro inhibitors. Bioorg. Med. Chem. Lett. **18:**5684–5688. http://dx.doi.org/10.1016/j.bmcl.2008.08.082.
24. **Kilianski A, Mielech A, Deng X, Baker SC.** 2013. Assessing activity and inhibition of MERS-CoV papain-like and 3C-like proteases using luciferase-based biosensors. J. Virol **87**(21):11955–11962.
25. **Roberts A, Deming D, Paddock CD, Cheng A, Yount B, Vogel L, Herman BD, Sheahan T, Heise M, Genrich GL, Zaki SR, Baric R, Subbarao K.** 2007. A mouse-adapted SARS-coronavirus causes disease and mortality in BALB/c mice. PLoS Pathog. **3:**e5. http://dx.doi.org/10.1371/journal.ppat.0030005.
26. **Chan KH, Chan JF, Tse H, Chen H, Lau CC, Cai JP, Tsang AK, Xiao X, To KK, Lau SK, Woo PC, Zheng BJ, Wang M, Yuen KY.** 2013. Cross-reactive antibodies in convalescent SARS patients' sera against the emerging novel human coronavirus EMC (2012) by both immunofluorescent and neutralizing antibody tests. J. Infect. **67:**130–140.
27. **Bolles M, Deming D, Long K, Agnihothram S, Whitmore A, Ferris M, Funkhouser W, Gralinski L, Totura A, Heise M, Baric RS.** 2011. A double-inactivated severe acute respiratory syndrome coronavirus vaccine provides incomplete protection in mice and induces increased eosinophilic proinflammatory pulmonary response upon challenge. J. Virol. **85:**12201–12215. http://dx.doi.org/10.1128/JVI.06048-11.
28. **Tseng CT, Sbrana E, Iwata-Yoshikawa N, Newman PC, Garron T, Atmar RL, Peters CJ, Couch RB.** 2012. Immunization with SARS coronavirus vaccines leads to pulmonary immunopathology on challenge with the SARS virus. PLoS One **7:**e35421. http://dx.doi.org/10.1371/journal.pone.0035421.
29. **Polack FP.** 2007. Atypical measles and enhanced respiratory syncytial virus disease (ERD) made simple. Pediatr. Res. **62:**111–115. http://dx.doi.org/10.1203/PDR.0b013e3180686ce0.
30. **Meyerholz DK, Griffin MA, Castilow EM, Varga SM.** 2009. Comparison of histochemical methods for murine eosinophil detection in an RSV vaccine-enhanced inflammation model. Toxicol. Pathol. **37:**249–255. http://dx.doi.org/10.1177/0192623308329342.
31. **Anthony SJ, Epstein JH, Murray KA, Navarrete-Macias I, Zambrana-Torrelio CM, Solovyov A, Ojeda-Flores R, Arrigo NC, Islam A, Ali**

Khan S, Hosseini P, Bogich TL, Olival KJ, Sanchez-Leon MD, Karesh WB, Goldstein T, Luby SP, Morse SS, Mazet JA, Daszak P, Lipkin WI. 2013. A strategy to estimate unknown viral diversity in mammals. mBio **4**(5):e00598-13. http://dx.doi.org/10.1128/mBio.00598-13.

32. **Menachery VD, Yount BL, Josset L, Gralinski LE, Scobey T, Agnihothram S, Katze MG, Baric RS.** 29 January 2014. Attenuation and restoration of SARS-CoV mutant lacking 2′ O methyltransferase activity. J. Virol. http://dx.doi.org/10.1128/JVI.03571-13.
33. **Wimmer E, Mueller S, Tumpey TM, Taubenberger JK.** 2009. Synthetic viruses: a new opportunity to understand and prevent viral disease. Nat. Biotechnol. **27:**1163–1172. http://dx.doi.org/10.1038/nbt.1593.
34. **Dormitzer PR, Suphaphiphat P, Gibson DG, Wentworth DE, Stockwell TB, Algire MA, Alperovich N, Barro M, Brown DM, Craig S, Dattilo BM, Denisova EA, De Souza I, Eickmann M, Dugan VG, Ferrari A, Gomila RC, Han L, Judge C, Mane S, Matrosovich M, Merryman C, Palladino G, Palmer GA, Spencer T, Strecker T, Trusheim H, Uhlendorff J, Wen Y, Yee AC, Zaveri J, Zhou B, Becker S, Donabedian A, Mason PW, Glass JI, Rappuoli R, Venter JC.** 2013. Synthetic generation of influenza vaccine viruses for rapid response to pandemics. Sci. Transl. Med. **5:**185ra168. http://dx.doi.org/10.1126/scitranslmed.3006368.
35. **Gierer S, Bertram S, Kaup F, Wrensch F, Heurich A, Krämer-Kühl A, Welsch K, Winkler M, Meyer B, Drosten C, Dittmer U, von Hahn T, Simmons G, Hofmann H, Pöhlmann S.** 2013. The spike protein of the emerging betacoronavirus EMC uses a novel coronavirus receptor for entry, can be activated by TMPRSS2, and is targeted by neutralizing antibodies. J. Virol. **87:**5502–5511. http://dx.doi.org/10.1128/JVI.00128-13.
36. **Huynh J, Li S, Yount B, Smith A, Sturges L, Olsen JC, Nagel J, Johnson JB, Agnihothram S, Gates JE, Frieman MB, Baric RS, Donaldson EF.** 2012. Evidence supporting a zoonotic origin of human coronavirus strain NL63. J. Virol. **86:**12816–12825. http://dx.doi.org/10.1128/JVI.00906-12.
37. **Donaldson EF, Sims AC, Graham RL, Denison MR, Baric RS.** 2007. Murine hepatitis virus replicase protein nsp10 is a critical regulator of viral RNA synthesis. J. Virol. **81:**6356–6368. http://dx.doi.org/10.1128/JVI.02805-06.
38. **Sims AC, Tilton SC, Menachery VD, Gralinski LE, Schäfer A, Matzke MM, Webb-Robertson BJ, Chang J, Luna ML, Long CE, Shukla AK, Bankhead AR, Burkett SE, Zornetzer G, Tseng CT, Metz TO, Pickles R, McWeeney S, Smith RD, Katze MG, Waters KM, Baric RS.** 2013. Release of severe acute respiratory syndrome coronavirus nuclear import block enhances host transcription in human lung cells. J. Virol. **87:**3885–3902. http://dx.doi.org/10.1128/JVI.02520-12.
39. **Matthews KL, Coleman CM, van der Meer Y, Snijder EJ, Frieman MB.** 17 January 2014. The ORF4b-encoded accessory proteins of MERS-coronavirus and two related bat coronaviruses localize to the nucleus and inhibit innate immune signaling. J. Gen. Virol. http://dx.doi.org/10.1099/vir.0.062059-0.
40. **Almazán F, Dediego ML, Sola I, Zuñiga S, Nieto-Torres JL, Marquez-Jurado S, Andrés G, Enjuanes L.** 2013. Engineering a replication-competent, propagation-defective middle East respiratory syndrome coronavirus as a vaccine candidate. mBio **4**(5):e00650-13. http://dx.doi.org/10.1128/mBio.00650-13.
41. **Scobey T, Yount BL, Sims AC, Donaldson EF, Agnihothram SS, Menachery VD, Graham RL, Swanstrom J, Bove PF, Kim JD, Grego S, Randell SH, Baric RS.** 2013. Reverse genetics with a full-length infectious cDNA of the Middle East respiratory syndrome coronavirus. Proc. Natl. Acad. Sci. U. S. A. **110:**16157–16162. http://dx.doi.org/10.1073/pnas.1311542110.
42. **Yount B, Roberts RS, Lindesmith L, Baric RS.** 2006. Rewiring the severe acute respiratory syndrome coronavirus (SARS-CoV) transcription circuit: engineering a recombination-resistant genome. Proc. Natl. Acad. Sci. U. S. A. **103:**12546–12551. http://dx.doi.org/10.1073/pnas.0605438103.
43. **Frieman M, Basu D, Matthews K, Taylor J, Jones G, Pickles R, Baric R, Engel DA.** 2011. Yeast based small molecule screen for inhibitors of SARS-CoV. PLoS One **6:**e28479. http://dx.doi.org/10.1371/journal.pone.0028479.
44. **Hirai A, Ohtsuka N, Ikeda T, Taniguchi R, Blau D, Nakagaki K, Miura HS, Ami Y, Yamada YK, Itohara S, Holmes KV, Taguchi F.** 2010. Role of mouse hepatitis virus (MHV) receptor murine CEACAM1 in the resistance of mice to MHV infection: studies of mice with chimeric mCEACAM1a and mCEACAM1b. J. Virol. **84:**6654–6666. http://dx.doi.org/10.1128/JVI.02680-09.
45. **Smits SL, de Lang A, van den Brand JM, Leijten LM, van IJcken WF, Eijkemans MJ, van Amerongen G, Kuiken T, Andeweg AC, Osterhaus AD, Haagmans BL.** 2010. Exacerbated innate host response to SARS-CoV in aged non-human primates. PLoS Pathog. **6:**e1000756.
46. **Zhao J, Zhao J, Legge K, Perlman S.** 2011. Age-related increases in PGD(2) expression impair respiratory DC migration, resulting in diminished T cell responses upon respiratory virus infection in mice. J. Clin. Invest. **121:**4921–4930. http://dx.doi.org/10.1172/JCI59777.
47. **Day CW, Baric R, Cai SX, Frieman M, Kumaki Y, Morrey JD, Smee DF, Barnard DL.** 2009. A new mouse-adapted strain of SARS-CoV as a lethal model for evaluating antiviral agents *in vitro* and *in vivo*. Virology **395:**210–222. http://dx.doi.org/10.1016/j.virol.2009.09.023.
48. **Consortium CSME.** 2004. Molecular evolution of the SARS coronavirus during the course of the SARS epidemic in China. Science **303:**1666–1669. http://dx.doi.org/10.1126/science.1092002.
49. **Sheahan T, Whitmore A, Long K, Ferris M, Rockx B, Funkhouser W, Donaldson E, Gralinski L, Collier M, Heise M, Davis N, Johnston R, Baric RS.** 2011. Successful vaccination strategies that protect aged mice from lethal challenge from influenza virus and heterologous severe acute respiratory syndrome coronavirus. J. Virol. **85:**217–230. http://dx.doi.org/10.1128/JVI.01805-10.
50. **Wecker M, Gilbert P, Russell N, Hural J, Allen M, Pensiero M, Chulay J, Chiu YL, Abdool Karim SS, Burke DS, HVTN 040/059 Protocol Team, NIAID HIV Vaccine Trials Network.** 2012. Phase I safety and immunogenicity evaluations of an alphavirus replicon HIV-1 subtype C gag vaccine in healthy HIV-1-uninfected adults. Clin. Vaccine Immunol. **19:**1651–1660. http://dx.doi.org/10.1128/CVI.00258-12.
51. **Slovin SF, Kehoe M, Durso R, Fernandez C, Olson W, Gao JP, Israel R, Scher HI, Morris S.** 2013. A phase I dose escalation trial of vaccine replicon particles (VRP) expressing prostate-specific membrane antigen (PSMA) in subjects with prostate cancer. Vaccine **31:**943–949. http://dx.doi.org/10.1016/j.vaccine.2012.11.096.
52. **Taylor KG, Paessler S.** 2013. Pathogenesis of Venezuelan equine encephalitis. Vet. Microbiol. **167:**145–150. http://dx.doi.org/10.1016/j.vetmic.2013.07.012.
53. **Reusken CB, Haagmans BL, Müller MA, Gutierrez C, Godeke GJ, Meyer B, Muth D, Raj VS, Smits-De Vries L, Corman VM, Drexler JF, Smits SL, El Tahir YE, De Sousa R, van Beek J, Nowotny N, van Maanen K, Hidalgo-Hermoso E, Bosch BJ, Rottier P, Osterhaus A, Gortázar-Schmidt C, Drosten C, Koopmans MP.** 2013. Middle East respiratory syndrome coronavirus neutralising serum antibodies in dromedary camels: a comparative serological study. Lancet Infect. Dis. **13:**859–866. http://dx.doi.org/10.1016/S1473-3099(13)70164-6.
54. **Wang N, Shi X, Jiang L, Zhang S, Wang D, Tong P, Guo D, Fu L, Cui Y, Liu X, Arledge KC, Chen YH, Zhang L, Wang X.** 2013. Structure of MERS-CoV spike receptor-binding domain complexed with human receptor DPP4. Cell Res. **23:**986–993. http://dx.doi.org/10.1038/cr.2013.92.
55. **Josset L, Menachery VD, Gralinski LE, Agnihothram S, Sova P, Carter VS, Yount BL, Graham RL, Baric RS, Katze MG.** 2013. Cell host response to infection with novel human coronavirus EMC predicts potential antivirals and important differences with SARS coronavirus. mBio **4**(3):e00165-13. doi: 10.1128/mBio.00165-13.